RESEARCH   **Open Access**

Seismic Strength Evaluation of Corroded Reactor Containment Building

Md Samdani Azad[1,4], Duy-Duan Nguyen[2], Bidhek Thusa[3,4] and Tae-Hyung Lee[4*]

Abstract

The purpose of this study is to investigate the effects of the corrosion phenomenon on the seismic strength of a reactor containment building (RCB) in nuclear power plants (NPPs). A corrosion degradation model is proposed based on the rationale of NPP structures and applied to the reinforcements near the base mat of RCB. Three corrosion levels associated with the service life of the structure up to 60 years are considered in this study. Seven different cases are considered depending on the location of corrosion. A series of pushover analyses are performed to evaluate the seismic responses of the corroded RCB, considering all cases with different levels of damage due to corrosion. The results are obtained in terms of global responses, in which capacity curves, base shear at different limit states, demand–capacity ratios, and reserve strength ratios (RSR) are quantified. The findings of this study demonstrate that corrosion can cause a reduction in structural capacity in terms of base shear of up to 19.5% during its service life of 60 years and that is dependent on how the corrosion is propagated within RCB. The results also illustrate that corrosion in the elements in the tension zone increases the sensitivity of the responses subjected to seismic loads.

Keywords Reactor containment building, Beam–truss model, Corrosion, Pushover analysis, Demand–capacity ratio, Reserve strength ratio

1 Introduction

The necessity of seismic performance assessments in nuclear power plant (NPP) structures is well established in the scientific society. In recent decades, it has become a critical issue for NPP structures, especially reactor containment building (RCB) structures. Scientists and researchers have imparted significant contributions to design codes and standards to improve the seismic performance evaluation frameworks and techniques.

*Correspondence:
Tae-Hyung Lee
thlee@konkuk.ac.kr
[1] Department of Civil and Environmental Engineering, Yonsei University, Seoul, South Korea
[2] Department of Civil Engineering, Vinh University, Vinh 461010, Vietnam
[3] Department of Civil and Environmental Engineering, Hanbat National University, Daejeon, South Korea
[4] Department of Civil and Environmental Engineering, Konkuk University, Seoul, South Korea

Seismic performance evaluation methods for RCBs have been proposed by several researchers in both deterministic and probabilistic manners (Holden et al., 2003; Na et al., 2008; Yang et al., 2009). Some researchers have discussed the damage performance and seismic fragility of containment buildings (Bao et al., 2020; Chen et al., 2021; Zheng et al., 2019). Since RCBs are in operating condition for many years, aging degradation can also raise concern and that can affect the seismic capacity of the existing structures.

Aging degradation is a common phenomenon for reinforced concrete (RC) structures. Corrosion in steel reinforcements is one of the predominant causes of damaging RC structures. Numerous studies have investigated the seismic performance of different infrastructures such as RC columns (Guo et al., 2015; Meda et al., 2014; Xu et al., 2020), moment-resisting frames (Liu et al., 2017), bridges (Cui et al., 2018; Zhong et al., 2012), and chimneys (Guo & Zhang, 2019). The outcomes of those studies showed

Azad *et al. Int J Concr Struct Mater* (2025) 19:6

Page 2 of 14

significant effects of rebar corrosion on the seismic performance of structures.

The corrosion phenomenon has also become a critical issue for NPP structures. Sandia National Laboratory (Cherry, 1996) performed a study on the corroded containment building and evaluated the degradation in the pressure capacity. Naus et al. (Naus et al., 1996) also studied the corrosion effect on containment structures and presented the consequences through a reliability framework. However, the studies are limited to liner and prestressed-tendon corrosion, and did not incorporate the effect of rebar corrosion. In recent years, several studies (Alhanaee et al., 2018; Matteo et al., 2021) considered the effect of rebar corrosion and computed the capacity of containment buildings. However, these studies are limited to the assessment of the pressure capacity.

The purpose of this study is to evaluate the seismic performances of the RCB structure accounting for the effects of reinforcing bar corrosions. The seismic performance of corroded RCB is evaluated using pushover analysis. The numerical models of RCBs' are developed in OpenSees using the beam–truss model (BTM). The understanding of the effect of reinforcement corrosion is developed in this study. Three damage states, which are the initiations of the cracking, yielding, and crushing, are defined and seven different cases are selected based on the corroded portion of RCB. The base shear capacity of RCB at different damage states is quantified for various corrosion levels including pristine and at 30 years, 45 years, and 60 years. The demand–capacity ratio is estimated and compared for different life spans. Another parameter, the reserve strength ratio (RSR), is proposed to understand the robustness of the degraded RCB. The differences in RSR values at different corrosion levels are addressed.

2 Numerical Model

2.1 Description of Case Study RCB
The reinforced concrete RCB designed in Korea is considered for numerical analyses in this study. RCB is a cylinder shear wall building where the radius of the cylinder is 23.5 m, the height is 54 m, and the thickness is 1.22 m. The radius of the dome is 23.2 m, and its average thickness is 1.07 m. The configuration of RCB and reinforcement details in the wall are shown in Fig. 1.

2.2 Modeling of Corrosion
Corrosion of the reinforcement is a serious deterioration mechanism for reinforced concrete structures. Corrosion can be modeled based on the damage mechanism of the low-carbon steel. Low-carbon steel is generally used in NPP structures (Naus et al., 1996). The damage due to corrosion can be modeled in terms of the loss of cross section or local pits or both. Corrosion is developed in
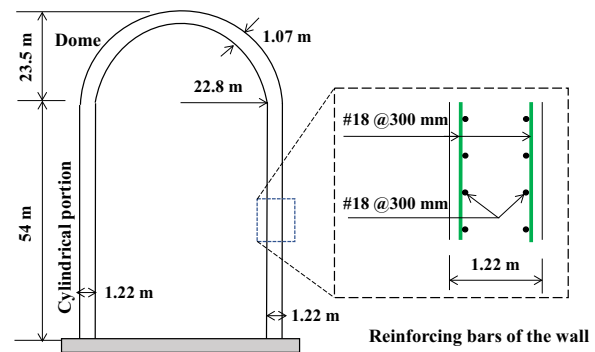

Fig. 1 Configuration of the case study RCB

two stages: the initiation and the propagation. The initiation of corrosion starts after several years of operations. The determination of a corrosion initiation is important for a proper estimation of a degradation of a structure over its lifetime. The initiation time depends on several factors including the perfection in construction and the external environment. There are several probabilistic models proposed by different researchers, mostly based on the chloride concentration, the critical chloride concentration, and the age factor (Karapetrou, 2015). Besides, these parameters include uncertainty as well. In addition, experimental data are required for a robust estimation of the corrosion initiation time. Due to the lack of experimental data, the corrosion initiation time is arbitrarily assumed as 15 years in this study.

The corrosion in the steel reinforcements starts to propagate after the initiation. There are several models available to compute the corrosion propagation over time. However, these models from previous studies were proposed for bridges' columns (Ghosh & Padgett, 2010) and no specific model is available for NPP structures. In this study, the rate of the corrosion propagation is assumed as 0.05 mm/years based on the illustrative example in an NRC report (Naus et al., 1996). Based on the assumption of corrosion initiation and corrosion rate, the corrosion model is utilized in terms of rebar area reduction as shown in Fig. 2a. The effects of the corrosion degradation of RCB are incorporated at the pristine condition, 30 years, 45 years, and 60 years, where the lifetime of NPP is assumed as 60 years based on the engineering judgment. The loss of the cross-sectional area of the reinforcing steel is 7%, 15%, and 23% at 30 years, 45 years, and 60 years, respectively. The corrosion degradation model is applied at the bottom part of the cylindrical wall, since it is considered as the most susceptible areas subjected to corrosion (Alhanaee et al., 2018). The corroded portion is located from the base mat to 25% height of the cylinder, as shown in Fig. 2b. Figure 2c–i shows various
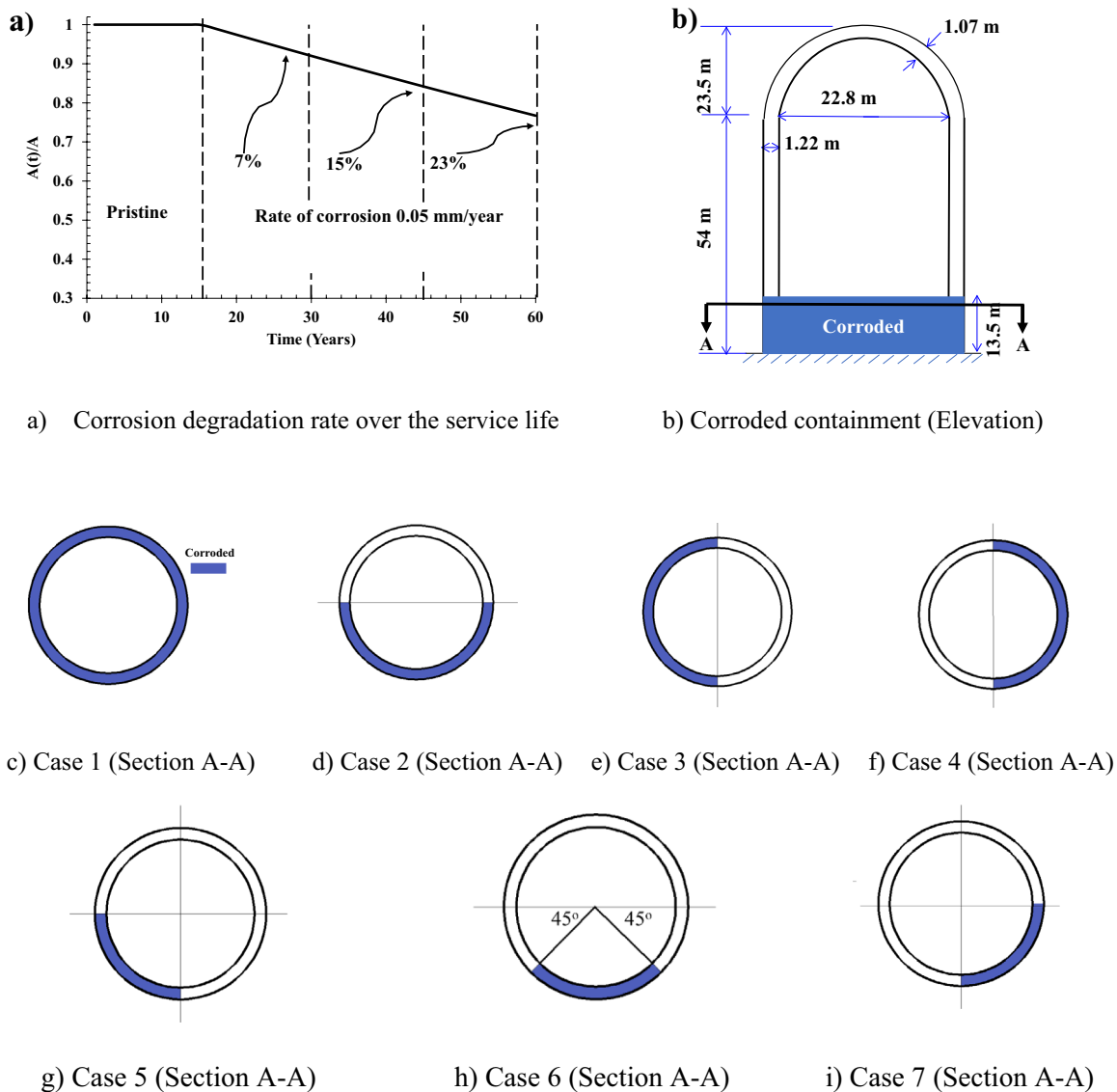
a)   Corrosion degradation rate over the service life

b) Corroded containment (Elevation)

c) Case 1 (Section A-A)   d) Case 2 (Section A-A)   e) Case 3 (Section A-A)   f) Case 4 (Section A-A)

g) Case 5 (Section A-A)   h) Case 6 (Section A-A)   i) Case 7 (Section A-A)

Fig. 2 Corrosion degradation and degraded containment sections

cases of corroded RCB. Figure 2c demonstrates case 1 where the RCB is assumed to be corroded along the full circumference near the base mat. Figure 2d–f illustrates the RCB with the half-circumferential corroded portion that considers three different directions from the loading direction. Figure 2g–i delineates RCB with a quarter-circumferential corroded portion with three different angular distributions. For all the cases, the height of the corroded portion is assumed to be one-fourth the height of the cylindrical portion, which is equivalent to 13.5 m.

2.3 Finite Element Model of RCB

For a seismic performance evaluation of NPP structures, several modeling techniques can be used such as lumped-mass stick model (LMSM), multilayer shell model (MLSM), three-dimensional finite element model using continuum elements (3D FEM), and beam–truss model (BTM). LMSM is a simplified approach, and it is not sufficient for nonlinear analyses, while 3D FEM and MLSM are computationally expensive (Nguyen et al., 2021). On the other hand, BTM is a relatively simplified and efficient model for performing nonlinear analyses, and it is employed for developing a numerical model of RCB in this study. The detailed advantages of BTM were

thoroughly discussed in Nguyen et al. (Nguyen et al., 2021).

A panel in BTM consists of two vertical and two horizontal elements, and two diagonal elements as shown in Fig. 3a. The dimension of a panel is determined based on the mesh convergence test (Nguyen et al., 2021). The length of the horizontal and vertical elements is set to 1.0 m. The horizontal and vertical elements are modeled as beam elements and the diagonal members are modeled as truss elements. The width of the beam elements is equal to the thickness of the wall, i.e., 1.22 m, while the height of the beams is set to the size of the panels. Besides, the width of the diagonal truss elements, *b*, is computed as the product of the length of the panel, *a*, and $\sin\theta_d$, as shown in Eq. (1).

$$b = a \times \sin\theta_d. \tag{1}$$

Here, θ_d is the angle between the diagonal and the horizontal elements which should be determined based on the strut-and-tie concept (Lu et al., 2014). RCB is modeled using OpenSees (Mazzoni et al., 2006), an open platform for earthquake engineering simulation, as shown in Fig. 3. The beam elements are constructed using the *forceBeamColumn* elements. The *corotTruss* element is used to develop the diagonal truss members. The vertical and horizontal beam elements are modeled considering the integration of the concrete and reinforcements, while the diagonal truss elements exhibit the behavior of pure concrete. The material models used to form beam and truss elements are nonlinear models. The *Concrete02* and *steel02* models are employed for the concrete and reinforcing bars, respectively. Figure 3 depicts the illustrative modeling of the RCB wall using BTM. The *concrete02* and *steel02* models are shown in Fig. 4. The material properties such as the density, tensile strength, and compressive strength of the containment concrete, and the yield strength and hardening ratio of the reinforcing bars are presented in Table 1. Corrosion is applied in terms of the reduction of the cross-sectional area of the reinforcement bars of both the vertical and horizontal members. As discussed earlier, the steel areas of the corroded portions are reduced to 7%, 15%, and 23% at 30 years, 45 years, and 60 years of service life.

2.4 Pushover Analysis

The pushover analysis or nonlinear static analysis is a reliable procedure to characterize the structural performance. The pushover analysis incorporates the nonlinear force–displacement behavior of local elements and the global performance of a structure subjected to monotonically increasing lateral loads. The base
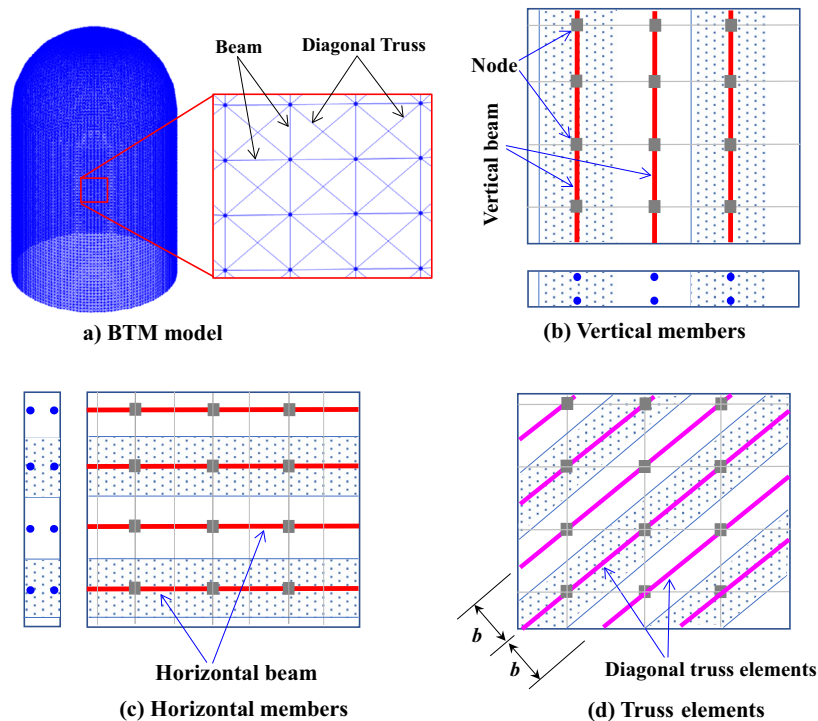

a) BTM model

(b) Vertical members

(c) Horizontal members

(d) Truss elements

Fig. 3 Numerical modeling of RCB using BTM

Azad *et al. Int J Concr Struct Mater*   (2025) 19:6
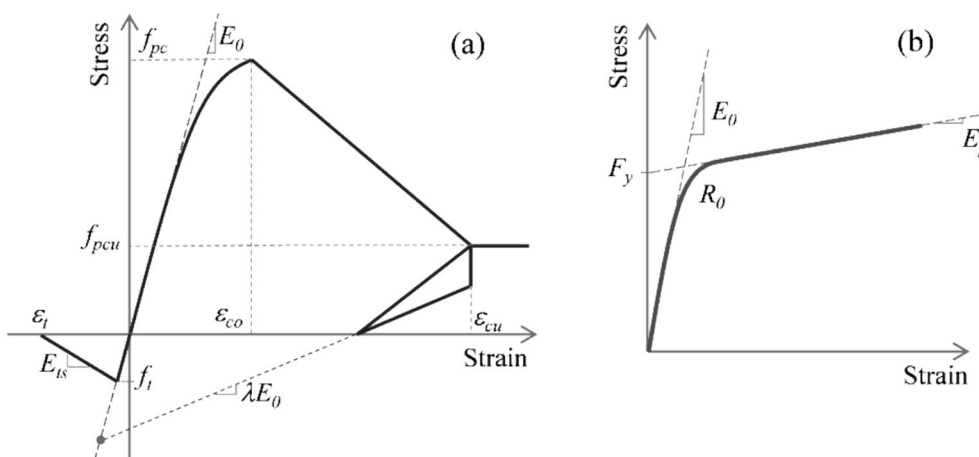
Page 5 of 14

Fig. 4 Constitutive models: **a** concrete and **b** reinforcing steel

Table 1 Material properties of RCB

Contents	Value
Density of concrete	2400 kg/m^3
Tensile strength of concrete	2.67 MPa
Compressive strength of concrete	45 MPa
Yield strength of steel	413 MPa
Hardening ratio of steel	0.01

shear–displacement curve is also known as the capacity curve where different damage states of the structure can be obtained.

In this study, a series of pushover analyses are conducted to determine the force–displacement relationships and the performance levels of the corroded RCB. Between force-control and displacement-control techniques, the latter is adopted in this study. An inverted triangular load distribution is applied for pushover analyses. The structure is pushed to 500 mm at the top level. The damage states are then defined based on the stress development in local fibers of element sections. Three damage states, which are initiations of cracking, yielding, and crushing, are demonstrated. The cracking and crushing are monitored in the concrete fibers while the yielding is monitored in the steel fibers. The damage state definition based on stress–strain relationships is illustrated in Fig. 5. It is depicted that the cracking in concrete initiates at first and is followed by the yielding of steel and crushing of concrete. The structure is considered collapsed if the first local element is subjected to crushing.

An effective parameter for the evaluation of seismic performances, namely the demand–capacity ratio (DCR), is obtained from pushover analyses. DCR is estimated according to the provision of ASCE 41−17 (American

Society of Civil Engineers, 2017a), expressed by the following equation:

$$\text{DCR} = \frac{Q_{\text{UD}}}{Q_{\text{CE}}}, \tag{2}$$

where Q_{UD} is the force caused by gravity and earthquake loads; Q_{CE} is the expected strength of the component or element. This study considers the strength at the crushing state for Q_{CE}.

2.5 Reserve Strength Ratio (RSR)

The reserve strength ratio (RSR) (Defranco et al., 2010; Refachinho et al., 2017) is an established parameter of robustness that is being used in offshore industries for decades. RSR is defined as the ratio between the base shear at structural collapse and characteristics of environmental loads (Refachinho et al., 2017). To the best of the author's knowledge, RSR has never been introduced in the assessment of NPP structures. RSR is a measure to understand the robustness of a structure after certain damage due to various corrosion levels including pristine and at 30 years, 45 years, and 60 years. The higher the value of RSR, the more robust is the structure.

The authors propose a strategy based on the behavior of local members of RCB. A schematic diagram of the evaluation of RSR is depicted in Fig. 6. At first, the weakest member, e.g. the member which will be crushing first, is identified. The stress–strain behavior of the weakest member is monitored. The peak stress is noted and the corresponding load step is recorded. Then the base shear capacity of the corresponding load step is observed. This base shear capacity is considered to evaluate RSR.

The value of this base shear is significant for this structure, since the concrete stress of the corresponding member starts to follow a descending branch. It illustrates that
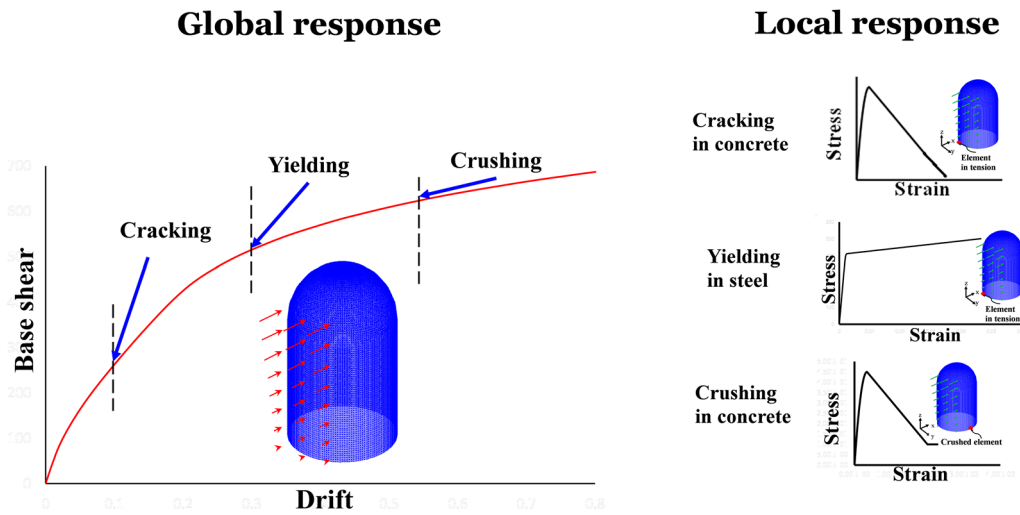
Azad *et al. Int J Concr Struct Mater*   (2025) 19:6

Page 6 of 14

Global response

Local response

Fig. 5 Definition of damage states on the pushover curve

the local member starts to lose its strength. The contribution and response of local members are important for this structure since small leakage can cause significant damage to the economy and environment. RSR can be evaluated by Eq. (3) after checking the base shear at the corresponding load step. The design earthquake load is calculated according to the provision of ASCE 41–17 (American Society of Civil Engineers, 2017a).

$$\text{RSR} = \frac{C}{V}, \tag{3}$$

where C is the peak structural capacity of the structure determined based on the peak stress of the local weakest member; V is the design earthquake load, which can

be calculated according to the provision of ASCE 4–16 (American Society of Civil Engineers, 2017b), expressed as

$$V = \alpha \cdot S_{\text{peak}} \cdot W, \tag{4}$$

where V is the static equivalent force or design base shear; $\alpha = 1$ is the dynamic amplification factor according to the provision of ASCE 41–17 (American Society of Civil Engineers, 2017a); $S_{\text{peak}} = 0.84g$ is the peak spectral acceleration from the design response spectrum and we have used NRC1.60 (US Nuclear Regulatory Commission, 2014) spectra in this case; W is the weight of the structure calculated from the FE-model.
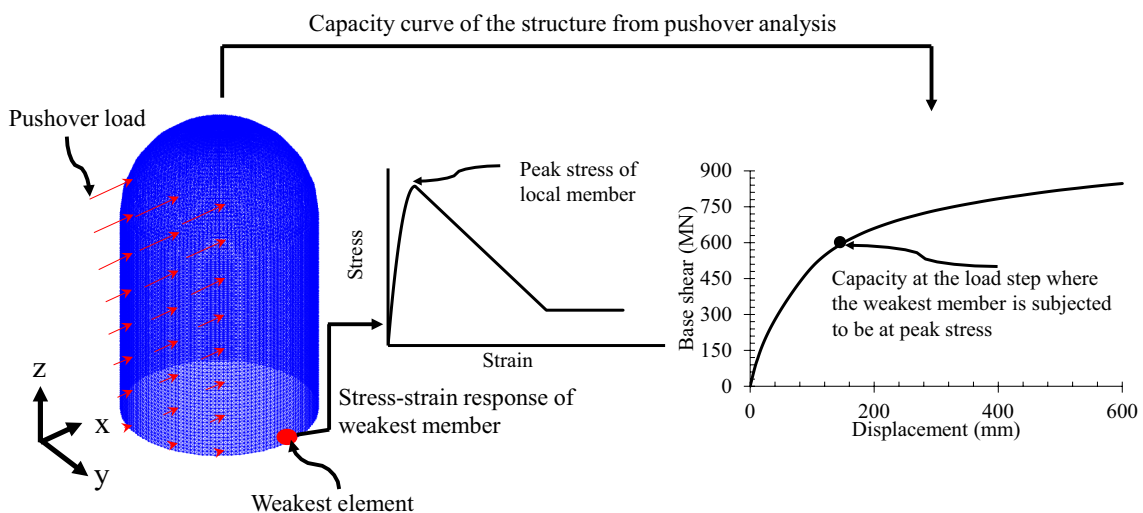
Fig. 6 Depiction of RSR for RCB

Azad *et al. Int J Concr Struct Mater* (2025) 19:6

Page 7 of 14

3 Seismic Performance of RCB

The seismic performance of RCB is evaluated using nonlinear static analyses. The variation of performances of RCBs with various corrosion levels are quantified using global responses of the structure. The base shear and displacement at different damages states and demand–capacity ratio and RSR are derived as the global responses from the pushover analysis.

3.1 Capacity Curves

RCB is modeled within the capability of OpenSees for the BTM modeling scheme. The lateral load distributions for pushover analyses are based on the relative displacements of the fundamental mode shape of the structures. It is approximately inverse-triangular over the height of the structure.

Figure 7 demonstrates the capacity curves as the shear force–displacement relationship of the RCB with seven different cases at pristine conditions, 30 years, 45 years, and 60 years. The base shear capacity reduces within a range of a lower extent to a higher extent based on the location of corrosion. In Fig. 8, the application of pushover load and detailed quantification of the reduction can be observed. Figure 8a shows the location of the weakest element, element in compression, and element in tension based on the local member response from pushover analysis. Further discussion on the responses of local elements is elaborated in the latter section of this study. Figure 8b describes the quantification of capacity curve reduction of the RCB subjected to pushover loads for all cases during its service life. For case 1, the capacity curve reduces to 4.13%, 9.05%, and 14.13% at 30 years, 45 years, and 60 years, respectively. For instance, for case 2, it reduces to 2.06%, 4.47%, and 7.12% at 30 years, 45 years, and 60 years, respectively. In case 3, the reduction percentage increases to 3.47%, 7.65%, and 11.64% at 30 years, 45 years, and 60 years of service life, respectively. In case 4, the reduction percentage is found to be 0.67%, 1.59%, and 2.84% at different intervals of service life, respectively. The corroded portion is present partially in both the tension zone and compression zone in case 2, while the tension zone is fully corroded in case 3. Furthermore, in case 4, corrosion is absent in the tension zone but fully present in compression. Based on the location of corrosion and tension zones in cases (2–4), it is clear that corrosion in the tension zone makes the structure more sensitive to seismic forces. The base shear capacity of structures is reduced due to the corrosion in the tension zone.

If we observe the reduction of the base shear for cases (5–7), it reduces to 1.71%, 3.71%, and 5.82% at 30 years, 45 years, and 60 years for case 5, respectively. The pushover curve reduction is 0.32%, 0.71%, and 1.22% at different stages of service life (i.e., at 30, 45, and 60 years) for case 6, respectively. Finally, case 7 demonstrates a reduction in the pushover curve of 0.67%, 1.59%, and 2.82% at the different levels of service life mentioned earlier, respectively. Moreover, the reduction of case 7 is almost identical to that of case 4, and corrosion in the elements of the tension zone is not present in both cases. The corroded portion is present partially in both the tension zones of case 5, while corrosion is missing in both the tension and compression zones of case 6. Case 7 has corrosion in the compression zone partially. Hence, it is confirmed that corrosion in the tension zone is significant for the seismic response of RCB. Figure 8b also shows the relative ranking of all the cases, with case 1 being the most sensitive and being followed by cases 3, 2, 5, case 4, case 7, and case 6 in that order.

3.2 Base Shear at Different Damage States

The base shears at cracking, yielding, and crushing of RCB are compared in Fig. 9 with various cases at different stages in its service life. The base shear (yielding and crushing) of cases 1, 2, and 4 is significantly reduced. Furthermore, case 5 demonstrates a decrease in the base shear at yielding, while the other cases show no significant drop in RCB capacity.

Figure 10 shows a more detailed quantification of the base shear capacity reduction. During the service life of RCB, all cases undergo a decrease in base shear at cracking, as shown in Fig. 10a. At 30, 45, and 60 years, the base shear at cracking of case 1 is reduced to 0.69%, 1.52%, and 2.32%, respectively. At 30 years, the base shear at cracking drops by 0.35%, 0.75% at 45 years, and 1.17% at 60 years in cases 2, 3, 4, and 7. Cases 5 and 6 delineate decreasing of the base shear at cracking of 0.17%, 0.37%, and 0.57% at 30, 45, and 60 years, respectively.

Figure 10b describes the reduction in base shear at yielding of all cases of RCB. The base shear capacity is reduced to 5.55%, 9.34%, and 15.19% at different lifetimes for case 1. Cases 2, 3, and 5 demonstrate base shear reductions within a range of (4.58–5.10)%, (8.19–10.43)%, and (13.82–14.83)% at 30, 45, and 60 years, respectively. Cases 4 and 6 show a very low amount of reduction in base shear at yielding. However, case 7 shows a higher reduction compared with cases 4 and 6, but a considerably lower reduction than cases 1, 2, 3, and 5.

Figure 10c depicts the reduction in the base shear at crushing strength of all cases of RCB. The base shear at crushing of RCB for case 1 decreases to 4.52%, 9.92%, and 15.41% at different ages, respectively. For case 3, the base shear capacity of the RCB lessens to 3.36%, 7.42%, and 11.78% at 30, 45 years, and 60 years, respectively. Cases 2, 4, and 5 show decrease in the base shear capacity of
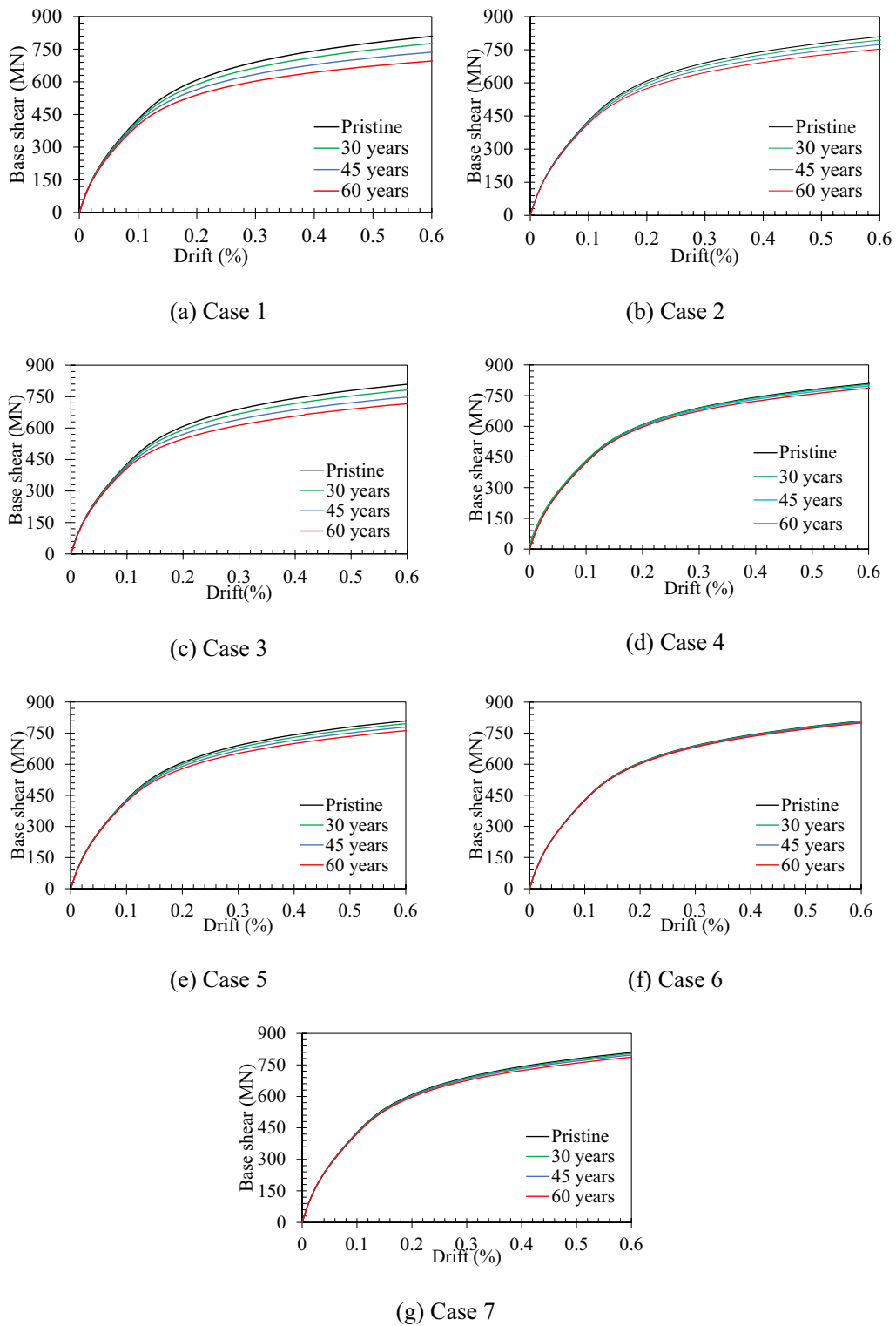
(a) Case 1

(b) Case 2

(c) Case 3

(d) Case 4

(e) Case 5

(f) Case 6

(g) Case 7

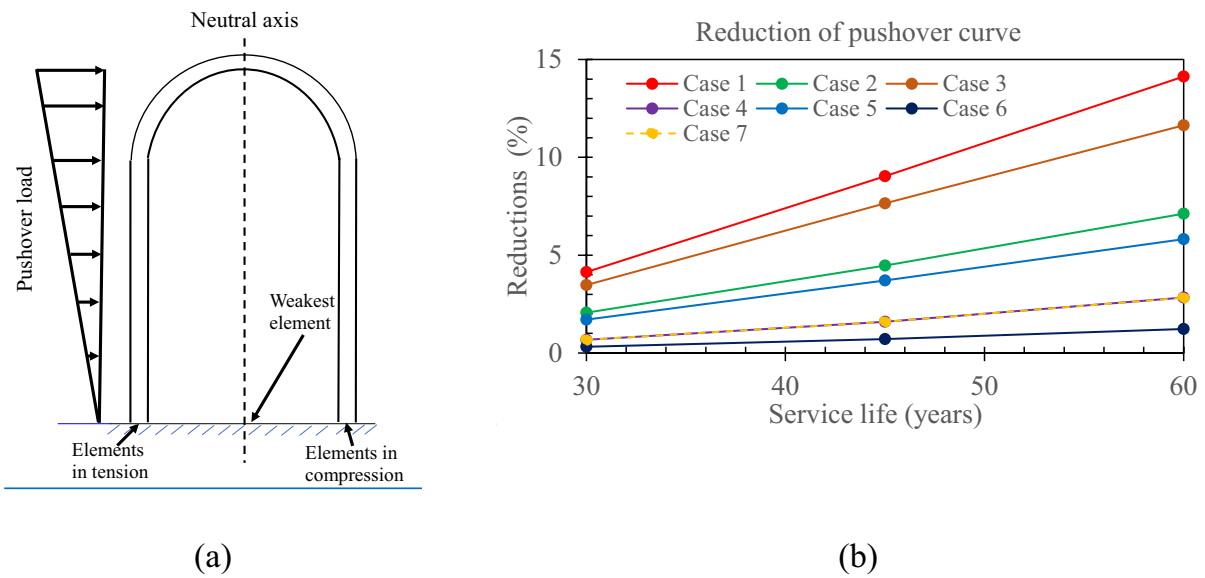**Fig. 7** Capacity curves of RCB with various corrosion levels in different cases

Fig. 8 **a** Elevation of RCB with pushover load, **b** reduction of pushover curve due to corrosion

(1.03–1.77)%, (2.48–2.80)%, and (4.53–5.68)% at 30, 45, and 60 years, respectively.

3.3 Demand–Capacity Ratio and Reserve Strength Ratio

The demand–capacity ratio based on ASCE 41–17 is shown in Fig. 11. The highest increase is shown in case 1, while case 3 also shows a significant increase in the demand–capacity ratio. Cases 2–5 show moderate increases, while cases 6–8 show only minor increases. In case 1, the demand–capacity ratio rises to 4.96%, 11.06%, and 18.32% after 30 years, 45 years, and 60 years, respectively. For case 3, the ratio exhibits an increment of 3.82%, 8.02%, and 13.36% at different intervals of service life. At 30 years, 45 years, and 60 years, the demand capacity ratio for cases 2, 4, and 5 increases to (1.15–1.92) %, (2.67–3.05) %, and (4.96–6.11) %, respectively. Even after 60 years of service life, the increments in cases 6 and 7 stay within 1.15%.

RSR of uncorroded and corroded RCBs is quantified in Fig. 12. RSR is a measure of robustness that demonstrates the condition and reduced capacity of RCB. Case 1 exhibits the greatest decrease, while case 3 indicates a significant drop in RSR. Cases 2, 4, and 5 demonstrate a moderate decrease, while cases 6 and 7 show only slight reductions. The RSR of case 1 diminishes to 4.65%, 9.97%, and 15.61% after 30 years, 45 years, and 60 years, respectively. For case 3, the ratio lessens to 3.99%, 8.64%, and 12.96% at different intervals of service life. RSR reductions of (0.33–1.66) %, (1.66–2.99) % and (2.99–4.65) % are found in cases 2, 4, and 5 during various service life intervals (i.e., 30, 45, and 60 years). Even after 60 years

of the service life, the increment for cases 6 and 7 is less than 1%.

4 Conclusions

This study evaluates the seismic performances of the RCB structure accounting for the effects of reinforcing bar corrosions. Four corrosion levels associated with the service life of the structure, which are pristine, at 30 years, 45 years, and 60 years, are considered in this study. The corrosion is assumed to be near the base mat and seven different cases are adopted concerning the direction and distribution of corroded elements. The numerical model of RCB is developed in OpenSees using the beam–truss model. A series of pushover analyses are performed to evaluate the seismic responses of the corroded RCB structure. The following conclusions are drawn based on numerical analyses.

- The effect of corrosion is negligible in the linear state based on the capacity curves since no significant reduction is noticeable even at the cracking stage.
- Corrosion in tension zones is sensitive for such structures subjected to pushover loads and the capacity of the RCB reduces to the greater amount in such cases.
- The significant effects are noticed for nonlinear behaviors, i.e., from the yielding to the crushing state. However, corrosion in tension zones is sensitive for such structures subjected to pushover loads, and the capacity of the RCB is reduced in such cases to a greater extent. It is dependent on the location of
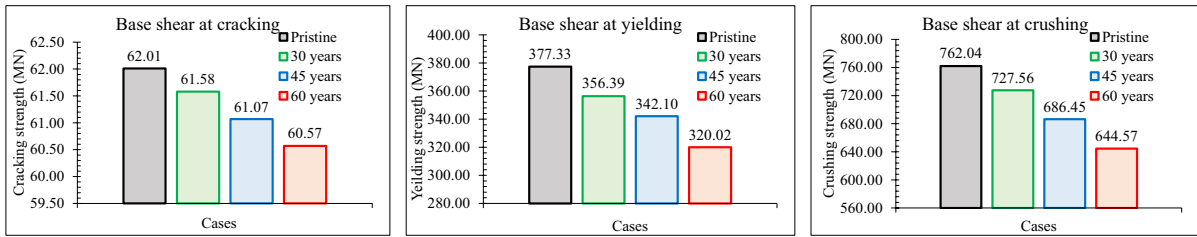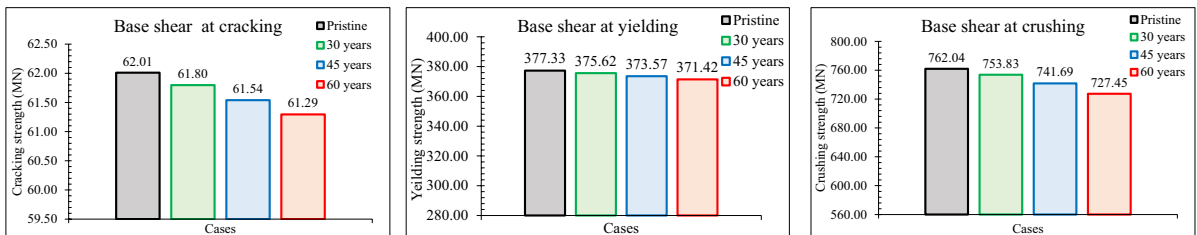
Case 1
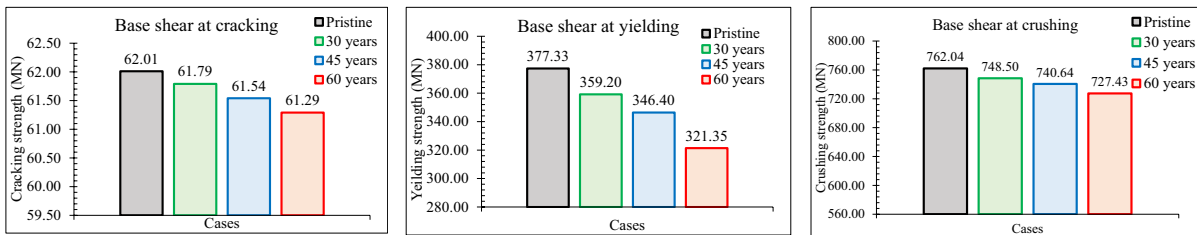
Case 2
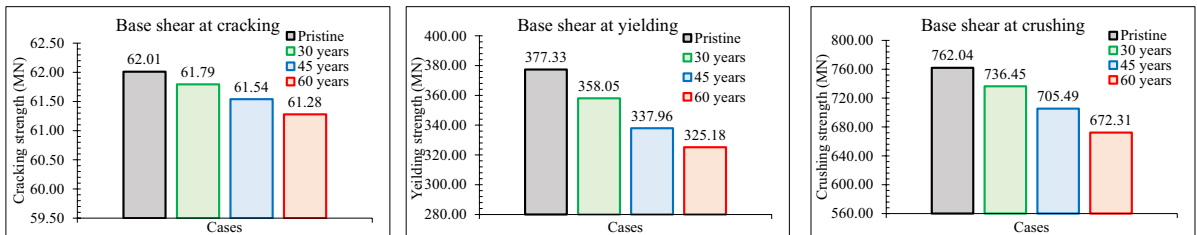
Case 3

Case 4

Fig. 9 Base shear capacity corresponding to damage states with various corrosion levels

corroded elements. Larger effects are reported if the corrosion is present in the tension zone.

- For performance-based design of NPP structures, the demand–capacity ratio is not only a simple quantification, but also an effective concept to the designer.
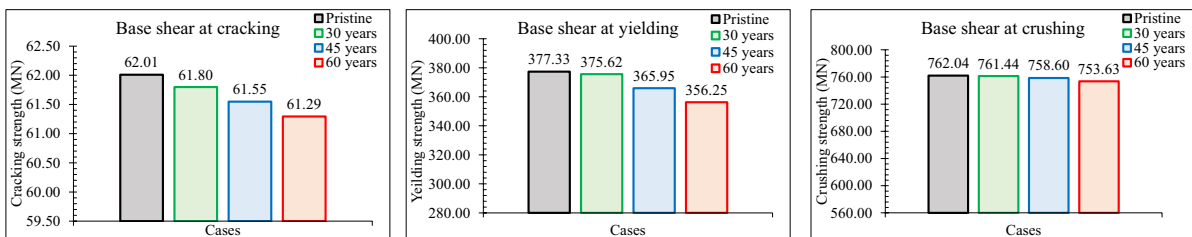
Compared with the results of pushover curves, the demand–capacity ratio exhibits a good agreement. Furthermore, the RSR values provide a rational estimation of the RCB's robustness, both uncorroded and corroded cases. Pushover curves and
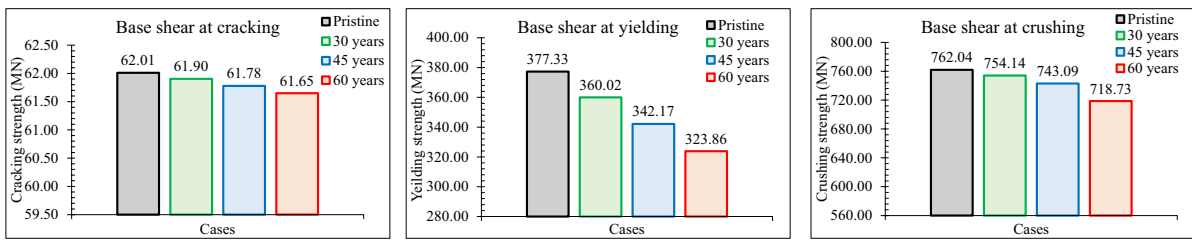
Case 5
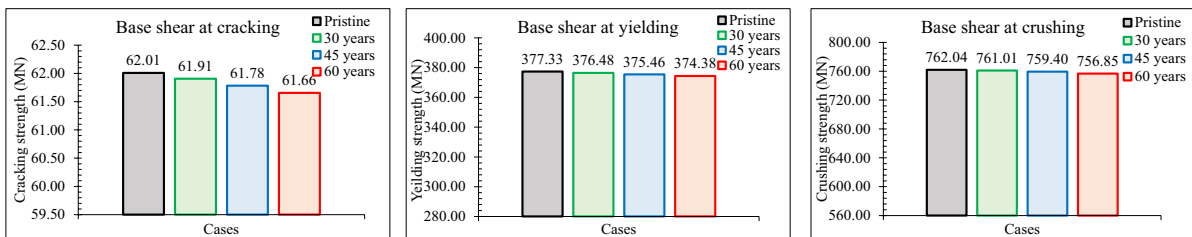
Case 6

Case 7

Fig. 9 continued

demand capacity ratios agree well with the RSR. Both demand–capacity ratio and the RCB's RSR are both affected by corrosion in tension zones.

The conclusions of this study are derived entirely from nonlinear static analysis and may not accurately reflect the behavior of the structure in dynamic circumstances. Hence, it is crucial to take into consideration these limitations when considering the findings of the study, which lack the complex and possibly influential dynamic impacts that may arise in real-life scenarios.
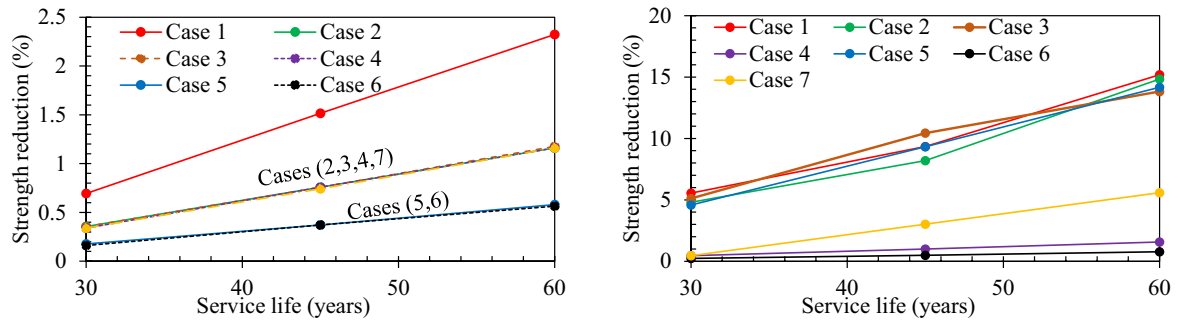
a) Base shear at cracking

b) Base shear at yielding
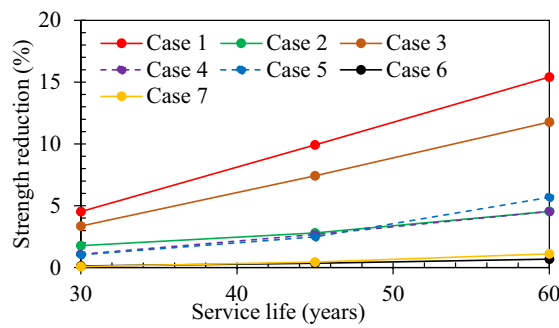
c) Base shear at crushing

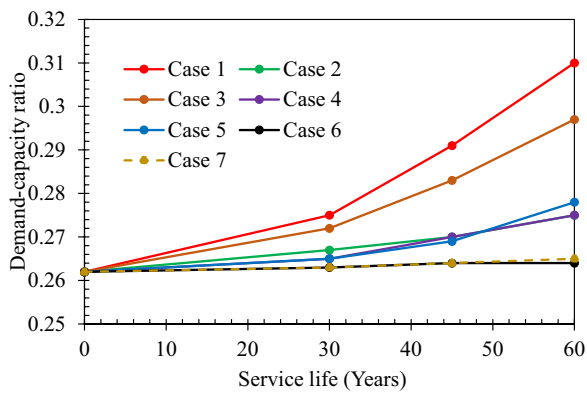**Fig. 10** Reduction of base shear capacity corresponding to damage states with various corrosion levels

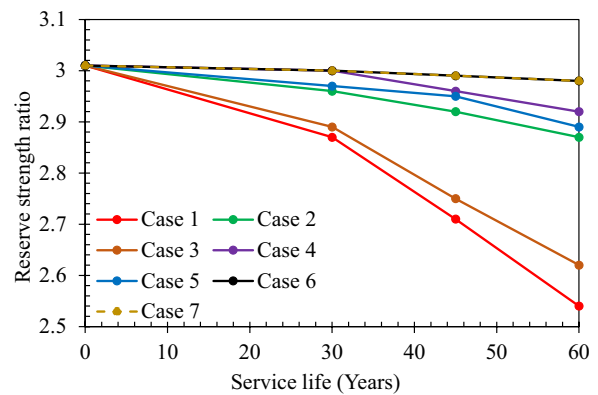**Fig. 11** The demand–capacity ratio of the RCB with different corrosion levels

Fig. 12 Reserve strength ratio of the RCB with different corrosion levels

Availability of data and materials
The datasets used and analyzed during the current study are available from the corresponding author on reasonable request.

Declarations

Competing interests
The authors declare that they have no competing interests.

References

Alhanaee, S., Yi, Y., & Schiffer, A. (2018). Ultimate pressure capacity of nuclear reactor containment buildings under unaged and aged conditions. *Nuclear Engineering and Design, 335*, 128–139.

American Society of Civil Engineers. (2017a). *Seismic evaluation and retrofit of existing buildings*. American Society of Civil Engineers.

American Society of Civil Engineers. (2017b). *Seismic analysis of safety-related nuclear structures*. American Society of Civil Engineers.

Bao, X., Zhai, C. H., Zhang, M. H., & Xu, L. J. (2020). Seismic capacity assessment of postmainshock damaged containment structures using nonlinear incremental dynamic analysis. *The Structural Design of Tall and Special Buildings, 29*(4), e1706.

Chen, W., Zhang, Y., & Wang, D. (2021). Damage development analysis of the whole nuclear power plant of AP1000 type under strong Main-aftershock sequences. *Nuclear Engineering and Design, 371*, 110975.

Cherry, J. L. (1996). *Analyses of containment structures with corrosion damage (No. SAND-96-0004C; CONF-961105-17)*. Sandia National Labs.

Cui, F., Zhang, H., Ghosn, M., & Xu, Y. (2018). Seismic fragility analysis of deteriorating RC bridge substructures subject to marine chloride-induced corrosion. *Engineering Structures, 155*, 61–72.

Defranco, S., O'Connor, P., Puskar, F., Bucknell, J. R., & Digre, K. A. (2010, January). *API RP 2SIM: Recommended practice for structural integrity management of fixed offshore platforms*. In Offshore Technology Conference. Offshore Technology Conference.

Ghosh, J., & Padgett, J. E. (2010). Aging considerations in the development of time-dependent seismic fragility curves. *Journal of Structural Engineering, 136*(12), 1497–1511.

Guo, A., Li, H., Ba, X., Guan, X., & Li, H. (2015). Experimental investigation on the cyclic performance of reinforced concrete piers with chloride-induced corrosion in marine environment. *Engineering Structures, 105*, 1–11.

Guo, X., & Zhang, C. (2019). Seismic fragility analysis of corroded chimney structures. *Journal of Performance of Constructed Facilities, 33*(1), 04018087.

Holden, T., Restrepo, J., & Mander, J. B. (2003). Seismic performance of precast reinforced and prestressed concrete walls. *Journal of Structural Engineering, 129*(3), 286–296.

Karapetrou, G. S. (2015). Seismic vulnerability of reinforced concrete buildings considering aging and soil-structure interaction effects (Doctoral dissertation, (No. GRI-2015-15565). Aristotle University of Thessaloniki).

Liu, X., Jiang, H., & He, L. (2017). Experimental investigation on seismic performance of corroded reinforced concrete moment-resisting frames. *Engineering Structures, 153*, 639–652.

Lu, Y., Panagiotou, M., & Koutromanos, I. (2014). Three-dimensional beam–#truss model for reinforced-concrete walls and slabs subjected to cyclic static or dynamic loading (No. PEER Report 2014/18).

Matteo, F., Carlo, G., Federico, P., & Enrico, Z. (2021). Time-dependent reliability analysis of the reactor building of a nuclear power plant for accounting of its aging and degradation. *Reliability Engineering & System Safety, 205*, 107173.

Mazzoni, S., McKenna, F., Scott, M. H., & Fenves, G. L. (2006). OpenSees command language manual. Pacific Earthquake Engineering Research (PEER) Center, 264.

Meda, A., Mostosi, S., Rinaldi, Z., & Riva, P. (2014). Experimental evaluation of the corrosion influence on the cyclic behaviour of RC columns. *Engineering Structures, 76*, 112–123.

Na, U. J., Chaudhuri, S. R., & Shinozuka, M. (2008). Probabilistic assessment for seismic performance of port structures. *Soil Dynamics and Earthquake Engineering, 28*(2), 147–158.

Naus, D. J., Oland, C. B., & Ellingwood, B. R. (1996). *Report on the aging of nuclear power plant reinforced concrete structures (No NUREG/CR-6424)*. Nuclear Regulatory Commission.

Nguyen, D. D., Thusa, B., Park, H., Azad, M. S., & Lee, T. H. (2021). Efficiency of various structural modeling schemes on evaluating seismic performance and fragility of APR1400 containment building. *Nuclear Engineering and Technology, 53*(8), 2696–2707.

Refachinho, M., Rigueiro, C., Martins, J. P., & Matos, R. (2017). Robustness, redundancy, and progressive collapse of fixed offshore structures. *Ce/papers, 1*(4), 539–553.

US Nuclear Regulatory Commission 1.60: Design Response Spectra for Seismic Design of Nuclear Power Plants. Regulatory Guide 1.60, Revision 2 (2014)

Xu, J. G., Wu, G., Feng, D. C., Cotsovos, D. M., & Lu, Y. (2020). Seismic fragility analysis of shear-critical concrete columns considering corrosion-induced deterioration effects. *Soil Dynamics and Earthquake Engineering, 134*, 106165.

Yang, T. Y., Moehle, J., Stojadinovic, B., & Der Kiureghian, A. (2009). Seismic performance evaluation of facilities: Methodology and implementation. *Journal of Structural Engineering, 135*(10), 1146–1154.

Zheng, Z., Zhai, C., Bao, X., & Pan, X. (2019). Seismic capacity estimation of a reinforced concrete containment building considering bidirectional cyclic effect. *Advances in Structural Engineering, 22*(5), 1106–1120.

Zhong, J., Gardoni, P., & Rosowsky, D. (2012). Seismic fragility estimates for corroding reinforced concrete bridges. *Structure and Infrastructure Engineering, 8*(1), 55–69.

Publisher's Note
Springer Nature remains neutral with regard to jurisdictional claims in published maps and institutional affiliations.

Md Samdani Azad　is currently a postdoctoral researcher at Yonsei University, Korea. He completed his PhD in civil engineering at Konkuk University, South Korea. His specialization is probabilistic seismic analysis of nuclear power plant structures, bridges, and fixed offshore structures, as well as the application of machine learning in the field of structural and earthquake engineering.

Duy-Duan Nguyen　is a lecturer at Vinh University in Vietnam with expertise in structural earthquake engineering and machine learning applications. He obtained his Ph.D. degree in Civil Engineering at Konkuk University, South Korea. His research spreads to the seismic performance evaluation of critical infrastructure, including nuclear power plant structures, tunnels, transmission towers, and bridges.

Azad *et al. Int J Concr Struct Mater*   (2025) 19:6

Page 14 of 14

Bidhek Thusa   is currently a postdoctoral researcher at Hanbat National University in Korea. He completed a Ph.D. in civil engineering at Konkuk University, South Korea. He has specialized in the artificial ground motion simulations and the seismic performance evaluation of nuclear power plant structures and prefabricated composite bridge systems.

Tae-Hyung Lee   is currently working as a Professor in the Department of Civil & Environmental Engineering, Konkuk University, Seoul, Republic of Korea. His expertise is probabilistic seismic analysis of nuclear power plant structures, bridges, LNG plants, and transmission towers. His contributions have been acknowledged on a national and worldwide scale, demonstrating his commitment to expanding our understanding of structural earthquake engineering.